REPORT DOCUMENTATION PAGE

Public reporting burden for this collection of information is estimated to average 1 hour per response, including the time for reviewing instructions, searching existing data sources, gathering and maintaining the data needed, and completing and reviewing this collection of information. Send comments regarding this burden estimate or any other aspect of this collection of information, including suggestions for reducing this burden to Department of Defense, Washington Headquarters Services, Directorate for Information Operations and Reports (0704-0188), 1215 Jefferson Davis Highway, Suite 1204, Arlington, VA 22202-4302. Respondents should be aware that notwithstanding any other provision of law, no person shall be subject to any penalty for failing to comply with a collection of information if it does not display a currently valid OMB control number. **PLEASE DO NOT RETURN YOUR FORM TO THE ABOVE ADDRESS.**

1. REPORT DATE (DD-MM-YYYY) November 11, 2006	2. REPORT TYPE Final Report	3. DATES COVERED (From - To) 6/1/02 – 5/31/06

4. TITLE AND SUBTITLE	5a. CONTRACT NUMBER
Micromechanics of Smart Materials for Large Deployable Mirrors	F49620-02-1-0252
	5b. GRANT NUMBER
	5c. PROGRAM ELEMENT NUMBER

6. AUTHOR(S)	5d. PROJECT NUMBER
Arup K. Maji	
	5e. TASK NUMBER
	5f. WORK UNIT NUMBER

7. PERFORMING ORGANIZATION NAME(S) AND ADDRESS(ES)	8. PERFORMING ORGANIZATION REPORT NUMBER
Department of Civil Eng. MSC01 1070 University of New Mexico Albuquerque, NM 87131	

9. SPONSORING / MONITORING AGENCY NAME(S) AND ADDRESS(ES)	10. SPONSOR/MONITOR'S ACRONYM(S)
Dr. Byung-Lip (Les) Lee Program Manager for Mechanics of Materials & 4015 Wilson Boulevard, AFOSR/NA, Room 713 Arlington, VA 22203-1954	
	11. SPONSOR/MONITOR'S REPORT NUMBER(S)

12. DISTRIBUTION / AVAILABILITY STATEMENT

Approved for Public Release, distribution is unlimited

AFRL-SR-AR-TR-08-0114

13. SUPPLEMENTARY NOTES

14. ABSTRACT

The objective of this research was to investigate the micro-mechanical behavior of a new type of smart material that could enable the accurate deployment of large sensors and structures in space, Elastic Memory Composites (EMC). The basic science aspect of this study involved understanding how the properties of the constituents (matrix and fiber) affect the deployment rate, deployment accuracy and failure of these smart composites. The experimental program and analytical model for deployment rate is presented first followed by that for the deployment accuracy and failure.

15. SUBJECT TERMS

16. SECURITY CLASSIFICATION OF:			17. LIMITATION OF ABSTRACT	18. NUMBER OF PAGES	19a. NAME OF RESPONSIBLE PERSON Arup K. Maji
a. REPORT	b. ABSTRACT	c. THIS PAGE	unlimited	16	19b. TELEPHONE NUMBER (include area code) 505-277-1757

MICROMECHANICS OF SMART MATERIALS
FOR LARGE DEPLOYABLE MIRRORS

Final Report

Submitted to:

Dr. Byung-lip Lee, AFOSR

Contract No: F49620-02-1-0252

by

Arup K. Maji
University of New Mexico
November 10, 2006

20080313326

Abstract:

The objective of this research was to investigate the micro-mechanical behavior of a new type of smart material that could enable the accurate deployment of large sensors and structures in space. Elastic Memory Composites (EMC) show promise as a structural material capable of providing its own, inherent deployment actuation. This shape memory effect is accomplished when the material is subjected to a specific thermo mechanical cycle. The partially thermoset epoxy matrix of this EMC is a viscoelastic polymer, which softens significantly at elevated temperature. Large geometric strains of up to 5 % are accommodated by this material via microbuckling of the fibers within this softened thermoset epoxy matrix. These large strains may be preserved, for later deployment, by returning the temperature of this composite to room temperature. Subsequent heating will release the stored strain energy of these fibers as the matrix compliance increases with temperature and time.

The basic science aspect of this study involved understanding how the properties of the constituents (matrix and fiber) affect the deployment rate, deployment accuracy and failure of these smart composites. The experimental program and analytical model for deployment rate is presented first followed by that for the deployment accuracy and failure.

Relevance:

An important aspect of a future National Missile Defense (NMD) system is improving the capability to perform reconnaissance from outer space. The ability to detect the launch of ICBMs and the ability to track it during its course is important to the success of any kinetic energy or directed energy (Laser) based mitigation. In order to achieve global coverage with improved resolution, larger space based mirrors are necessary. It is envisioned that a small number (4-6) of satellites (with sensors) can provide global coverage from orbits in the range of 10,000 miles, as opposed to the need for >50 satellites to do the same from Low Earth Orbit (LEO $\approx$ 300 miles). Reflectors larger than 10meters in diameter are desirable for such missions. Also, the greater energy demand in space necessitates large solar panels which can be adequately deployed with minimal weight and cost.

The Hubble Space Telescope is roughly 2.4 meters in diameter and weighs above 200kg/m. The largest launch vehicles (rockets) that will be available would not carry anything larger than 5 meters in diameter (including the new Enhance Expendable Launch Vehicle, EELV that is being built). Therefore, increasing the size of reflectors beyond 5meters would require deployable telescopes, which would be stowed during launch and deployed in space. Stowing and deploying large structures to optical levels of precision ($\lambda/30$, at wavelength $\lambda = 0.63$micrometers) is a major scientific challenge and requires basic understanding of material behavior at the microscopic level.

DEPLOYMENT RATE PREDICTION MODEL

Research Objectives:

- Develop a highly repeatable laminate fabrication process for low fiber volume fraction parts to be used in the upcoming test matrix
- Develop an experimental method for non-contact acquisition of deployment rate data from fabricated test coupons
- Experimentally characterize the constitutive relationship for the viscoelastic thermoset resin.
- Develop a deployment rate model for elastic memory composites

Sample Fabrication:

The EMC resin was obtained from Composite Technology development (CTD Inc.) of Lafayette, CO[1]. As an experimental resin, DP 5.1 was not, and is still not available in a prepreg cloth. Since a wet layup method was necessary, a woven IM7 fiber cloth was selected in order to maintain fiber orientation during the layup process. This cloth (Textile Products, Style 4375), however, was too tightly woven for the use of RTM for the given room temperature viscosity of the resin. A manual wet layup process was necessary.

It is widely understood that a resin reaches its lowest viscosity during the initial temperature ramp of the cure cycle. The faster the ramp, rate the lower the viscosity during this time frame. Viscosity decreases of up to three orders of magnitude may occur depending upon this ramp rate[2]. It was also observed that the shims and the capillary effect within the fibers were not sufficient to hold back enough resin to properly wet all the fibers. A rubber gasket was developed that would hold back the resin and allow for complete wetting of the fibers. Outside of this gasket, 0.050 inch shims were used to obtain a uniform laminate thickness. Porous peel ply provided a breathing path for the trapped air to escape during consolidation. The resin added to fill the vacant volume within the cavity formed by the gasket and caul plates, was determined from the difference between the cavity volume and the fiber volume. This resin was poured outside and between each of the three plies of IM7 fiber, plain weave cloth. Figure 1 illustrates this wet layup process, while the cured laminate is shown in Figure 2.
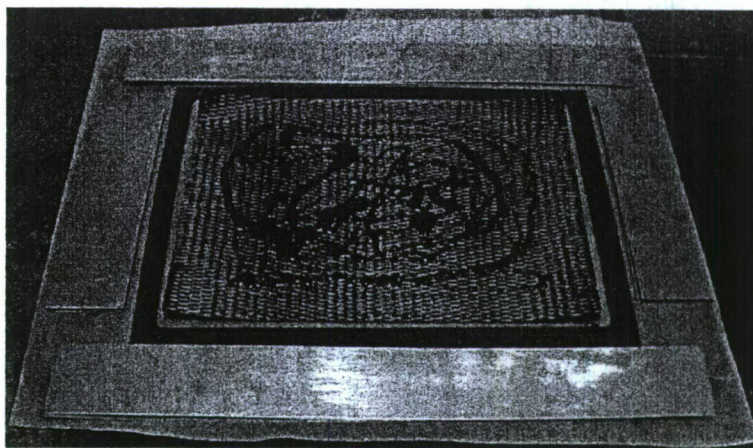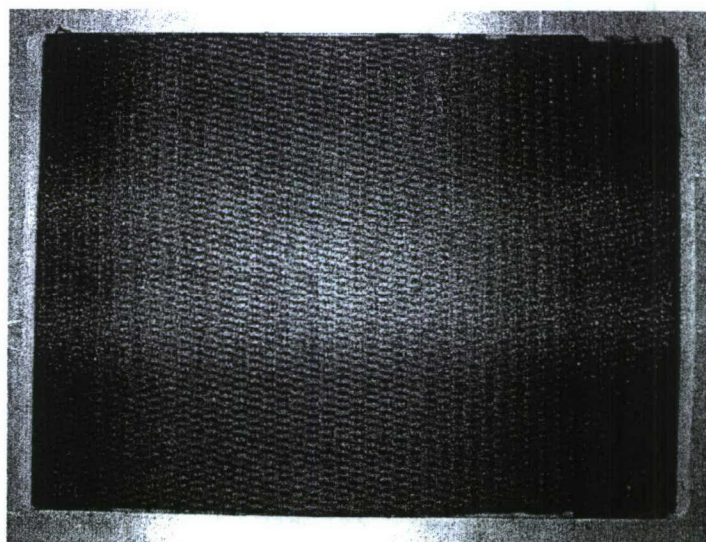
Figure 1 – Laminate wet layup process.

Figure 2 – Cured Laminate.

Neat resin specimens were required for characterization of the resin phase of this EMC. A mold was fabricated out of silicone rubber. This mold was then used to form three of the four surfaces of these neat resin specimens as shown in Figures 3 and 4. The fourth surface of these specimens was machined following the cure cycle to produce very high quality specimens. The autoclave shown in Figure 5 was used to cure both the laminates and neat resin specimens required for these studies.
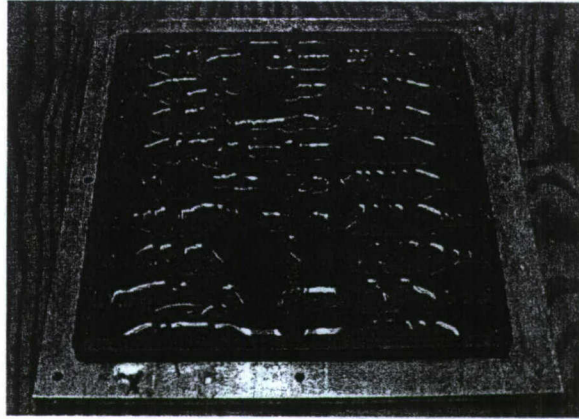
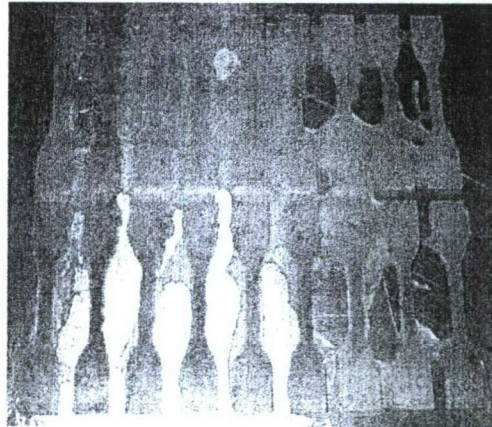Figure 3 – Poured neat resin specimens.

Figure 4 –Neat resin specimens, following the cure cycle.

Figure 5 – Neat resin specimens (background) and EMC laminate (forground) being placed in the autoclave for cure.

Experimental Deployment Rate:

In order to capture the observed deployment rate of this EMC material, two separate programs were written in LabVIEW. The first program captured video frames (of the deployment) synchronously with the corresponding run time and specimen temperature. These frames were compiled in an AVI video file. The second program accessed the video file and executed a pattern recognition routine to find two targets that were affixed to the free end of the deploying laminate. The Cartesian Coordinates of each target were output to a spreadsheet. These two points in the focal plane define a line whose angle changes from frame to frame. This changing angle as a function of time provides the desired validation data for the model. A visual indication of this pattern recognition process for one of these targets is shown in Figure 6.

Figure 6 – Optical Pattern recognition.

Viscoelastic Characterization:

Composite Technology Development (CTD) has developed a number of shape memory resins with varying chemical compositions. A specific CTD resin system, DP 5.1, has been selected as a constituent for this research. The viscoelastic character of this thermoset epoxy resin dictates the deployment rate of the EMC.

The experimental setup shown in Figure 7 was used to perform creep tests on DP 5.1 neat resin specimens prepared in accordance with ASTM 638-03. A laser extensometer was used to measure displacement after validating its accuracy against that of a conventional displacement transducer. Conventional transducers and clip-gages were not accurate for measurements on the soft resin matrix at elevated temperatures. These creep tests were performed at a variety of temperatures from 80 to 170°F. The resulting creep compliance curves were then subsequently shifted and trimmed to produce the master curve shown in Figure 8. This master compliance curve combined with the applied shift factors as a function of temperature produce a compliance function that is a function of both time and temperature.
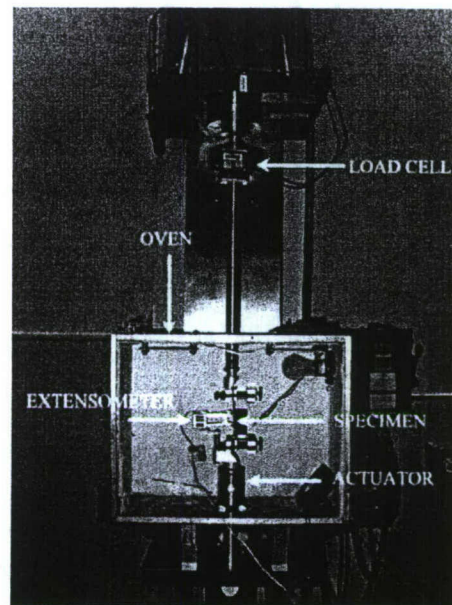
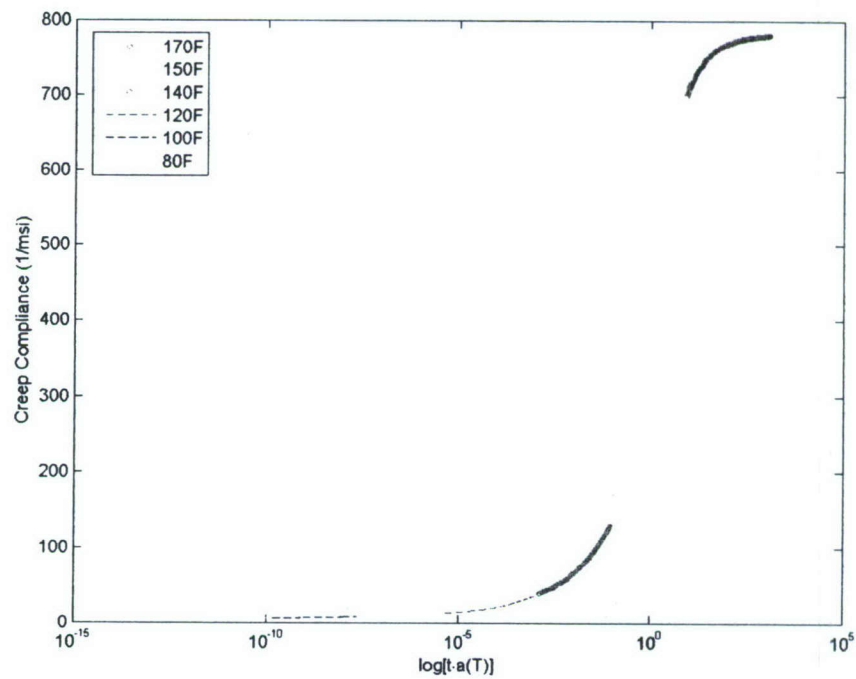Figure 7 – Experimental setup for the creep viscoelastic characterization tests.

Figure 8 – Assembled creep compliance master curve.

Deployment Rate Model:

The fundamental concept behind this deployment rate model is stepwise one dimensional equilibrium between the resin and fiber phases as the resin softens with time or temperature. The fiber phase zero strain state is in the as cured state or the zero degree position. The zero strain state of the resin during deployment is assumed to be when at the beginning of deployment or the 180 degree position. The strain – curvature relationships for both phases are provided in Equations (1) and (2) aided by Figure 9.

$$\varepsilon_f(t) = -\frac{z}{\rho(t)} \tag{1}$$

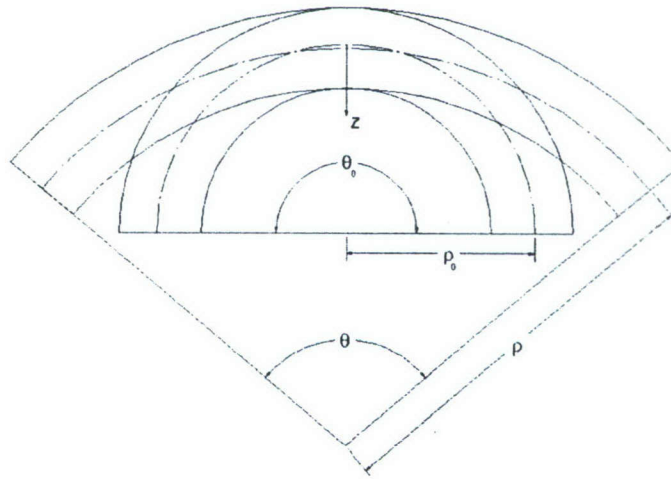$$\varepsilon_r(t) = z\left(\frac{1}{\rho_o} - \frac{1}{\rho(t)}\right) \tag{2}$$

Figure 9 – Deployment geometry used in strain – curvature relationship.

At the beginning of deployment the fibers within the composite are at their most buckled state. As the deployment progresses, the fibers straighten increasing the modulus of this phase until the axial modulus of the fiber is reached. The constitutive relationship which describes this process is given by Equation (3).

$$\sigma_f(t) = E_f(t)\varepsilon_f(t) \tag{3}$$

The resin phase constitutive relationship in terms of the creep compliance is:

$$\sigma_r(t,T) = \frac{\varepsilon_r(t)}{J_c(t,T)} \qquad (4)$$

Since both temperature and time are proportional to the creep compliance of the resin phase, when either or both of these quantities increase the equilibrium deployment angle decreases. Taking into account the geometry of this curved specimen during deployment the following relationship describes the deployment:

$$\theta(t) = \frac{\theta_o}{1 + J_c(T,t)E_f(t)} \qquad (5)$$

An initial indication of this model's validity is provided in Figure 10. The theoretical and experimental data sets presented in this Figure demonstrate good qualitative and quantitative agreement.
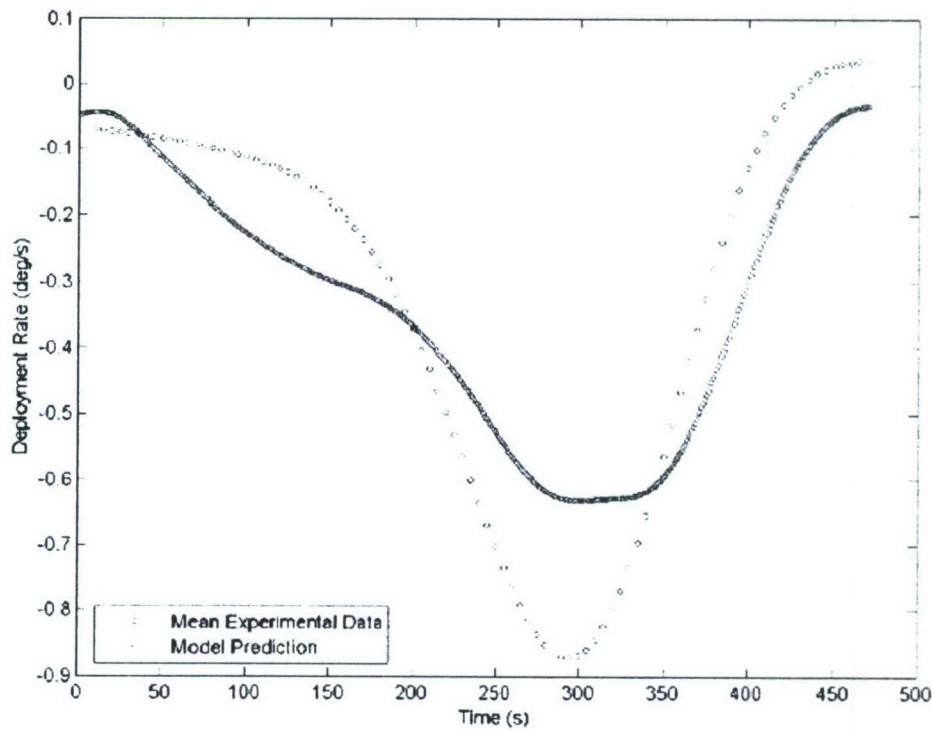

Figure 10 – Test data and Model prediction for deployment rate

DEPLOYMENT ACCURACY AND FAILURE

The limiting factor that dictates the deployment accuracy of this material is the micro-buckling of the individual fibers. The kinematics of this micro-buckling dictates whether or not the laminate behaves elastically, or if fibers break. This report presents the experimental methods used to characterize the deployment repeatability and performance of an EMC laminate as well as the fiber level effects of repeated deployment.

Research Objectives:

- Quantify the deployment accuracy. In the case of a hinge folded through a known radius of curvature (angle), this can be quantified as an "un-recovered" angular value, which can then be interpreted as a % recovery of the original induced angle.
- Obtain a relationship between material property degradation and both induced packaging strain and repeated deployment cycles.
- Obtain an analysis method that allows a designer to obtain an approximate upper limit for the maximum amount of curvature that a laminate can achieve given fiber and resin properties.

Testing and Results:

The EMC test material consisted of 12 8"x1" unidirectional coupons with a fiber volume fraction of 40%. The twelve coupons were evenly split between two-ply and four-ply laminates. The laminates were reinforced with T300 carbon fibers, and the matrix material was DP-7 EMC resin, which is an epoxy based thermoset resin [3]. This resin had a glass transition temperature of approximately 70°C. Testing was conducted at 100°C to ensure that bending was done within the full soft-resin state of the polymer.

The deployment precision study involved characterizing both the deployment precision of the EMC coupons at varying bending strains under near-zero resistance as well as the deployment repeatability due to increasing bending and deployment cycles. The primary variable for this test was the bend ratio, β, or the ratio of bend radius to material thickness, which is also inversely related to the maximum effective strain[4].

$$\beta = \frac{t}{R} = \frac{1}{\varepsilon_{eff}} \tag{6}$$

Tests were conducted at bend ratios of 2.5, 5, 10, 20, 40, and 80. All possible bend ratio combinations are shown in Table 1 based on the material thickness and bend radius of the test fixtures. Each deployment test was also conducted a total of 5 times in order to characterize the material's deployment repeatability performance. Figure 11 shows the test fixture that was used for the non-tension tests.

Laminate Thickness	Bend Radius				
	0.125"	0.25"	0.5"	1.0"	2.0"
(2-Ply) 0.025"	5	10	20	40	80
(4-Ply) 0.05"	2.5	5	10	20	40

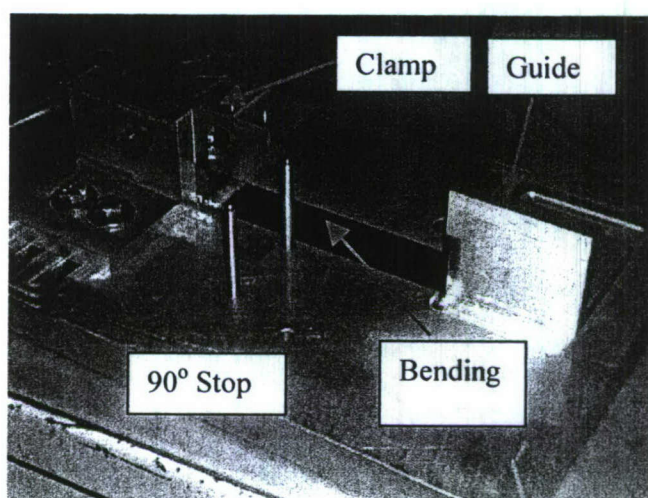Table 1: Deployment Precision Test Matrix

Figure 11- Non-Tension Bending Apparatus

The results from the non-tension tests are shown in Figure 12. The data does not reveal a discernable trend although the % recovery does fall within a range of approximately +/- 2%, which is considered very encouraging. However, the occurrence of over-deployment or, % recovery exceeding 100%, was not expected.
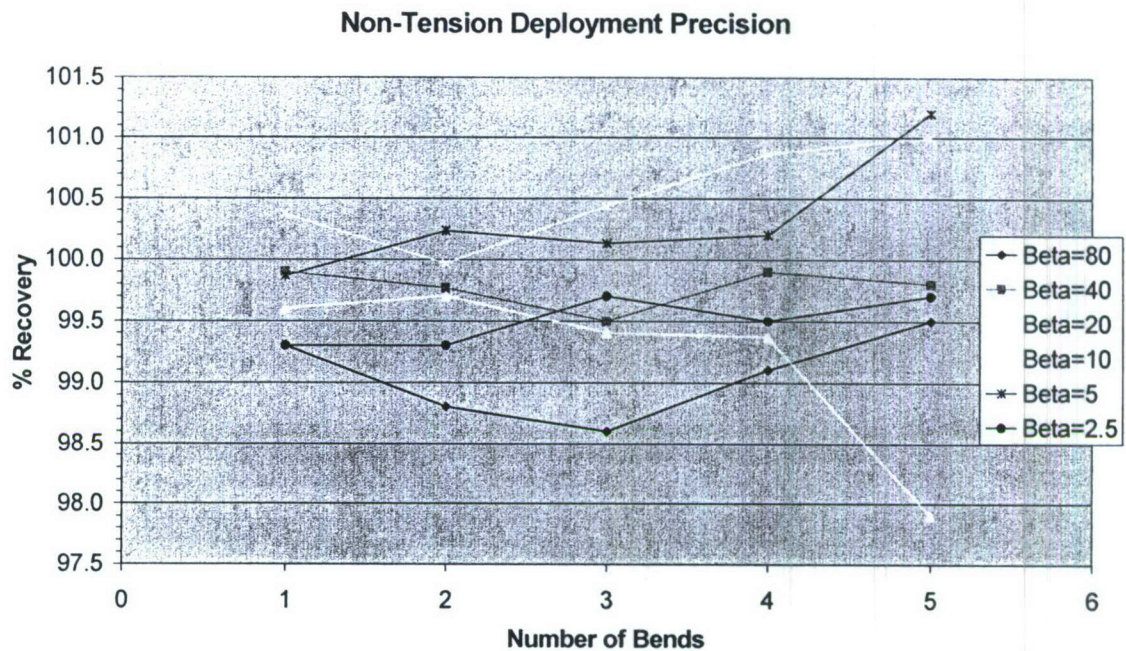
Non-Tension Deployment Precision

Figure 12- Non-Tension Deployment Precision Results

Fiber Damage Investigation:

Each coupon was inspected using an optical microscope following the completion of the deployment precision and repeatability tests. This investigation revealed observable damage in only those coupons tested at bend ratios of 20 (ε_{eff}=0.05) or less. Additionally, fiber damage was only observed on the compression side of the bend. In-plane micro-buckling was only observed in the $\beta = 20$, non-tension test, which is shown in Figure 3. However, fiber fracture was observed in the tension test at the same bend ratio. Based on this difference, it was assumed that the minimum achievable bend ratio without fiber damage was 20. Therefore according to Equation 6, the critical effective strain, or the effective strain at which fiber fracture occurs, is 0.05. It should also be noted that it was originally theorized that the application of tension during bending decreases fiber damage, which is counter to this result.

The in-plane micro-buckle shown in Figure 13 can be quantified using the T300 fiber's known diameter of 8 microns. Using this constant, an approximate micro-buckle wavelength and amplitude range of 0.64-0.40mm and 0.088-0.048mm respectively was obtained. It should be noted that a wavelength is defined here as one-half of a sine curve, or the distance between two inflection points.
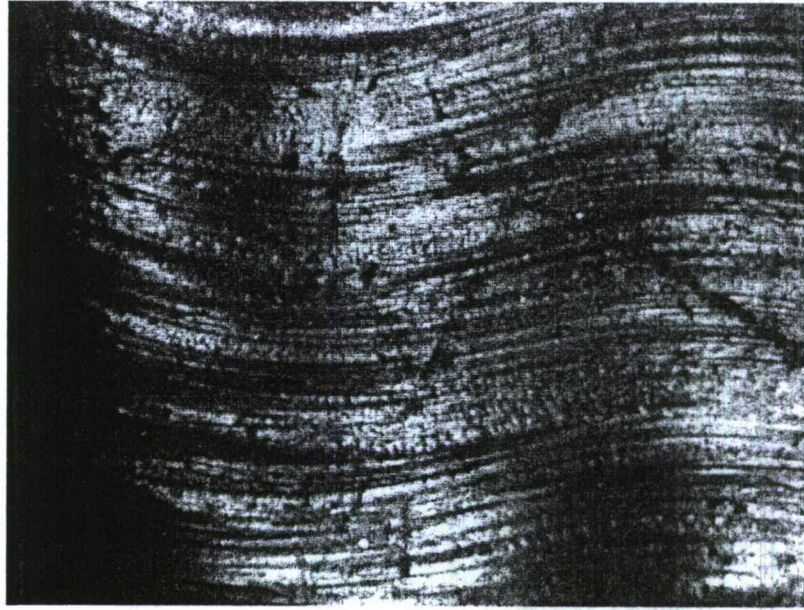
Figure 13- In-Plane Micro-Buckling in the $\beta = 20$, Non-Tension Test

Kinematic Analysis[4]:

As previously stated, the goal of this analysis is to obtain an approximation for the maximum effective strain an EMC laminate can achieve given fiber and resin properties. The end result was a two-fold analysis consisting of both a stability and kinematic analysis with a related intermediate variable defined here as the critical wavelength or, the minimum wavelength a fiber can achieve prior to fracture. The critical wavelength, λ_{cr}, is a material property based on the fiber's failure strain.

Equation 7 shows the relationship between the effective strain and the wavelength to amplitude ratio for a sinusoid if the axial strain is neglected[3].
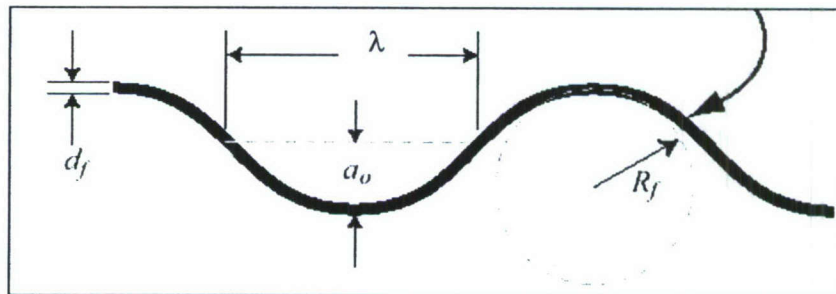

Figure 14- The Sinusoid Profile of a Micro-Buckled Fiber

$$\varepsilon_{effective} = \frac{1}{1 + \frac{4}{\pi^2}\frac{\lambda^2}{a_o^2}} \qquad (7)$$

Equation 7 (see Figure 14 for the relevant terminology) results in an effective strain range of 3.4 to 4.5% based on the observed range of the amplitude to wavelength ratio, which may be considered reasonably close to the approximated value of 5% based on the inverse of the bend ratio. Additionally, one would expect Equation 6 to over predict the effective strain since it neglects the contribution from the tension fibers.

The maximum achievable curvature for T300 fibers is 0.40mm obtained assuming an r_f of 4 microns and an ε_{fail} of 0.01. The kinematic relations[3] results in a wavelength of 0.58mm assuming that the effective failure strain corresponding to the minimum achievable curvature is 0.05. This wavelength clearly falls within the observed range of 0.64 to 0.40mm.

Stability Analysis:

Much of this analysis is based on Timoshenko's solution for the buckling load of a bar on an elastic foundation[5]. Timoshenko's solution models the elastic medium as a series of axial members with a certain spacing and stiffness. He derives expressions for both the strain energy due to bending of a bar with stiffness EI and length l, and ultimately derives an expression shown in Equation 8 for the critical load for this column or, the load at which buckling of the bar occurs.

$$P_{cr} = \frac{\pi^2 EI}{l^2}\left(m^2 + \frac{\beta_n l^4}{m^2 \pi^4 EI}\right) \qquad (8)$$

The variables m and β_n refer to the number of half sine waves in the buckled shape and the stiffness of the foundation respectively. A similar energy method is now used to obtain approximations for both the value of β_n for a fiber within a laminate and ultimately the maximum achievable micro-buckle magnitude based on the laminate's material properties.

Shearing occurs between fibers of adjacent layers as a result of the varying bending strain through the laminate's thickness. It can be shown that the shear energy per unit length for this element is represented by Equation 9 where δ is the distance between adjacent fibers, G is the resin's shear modulus, and t is the thickness of the laminate.

$$U_1 = \frac{1}{2}\left(\frac{a_n}{t}\delta\right)^2 G \qquad (9)$$

The energy equations can now be minimized with respect to the buckled shape, m, to obtain the wavelength corresponding to the lowest energy mode. The results can be simplified with the terms rearranged to show that Equation 10 represents the critical micro-buckle wavelength.

$$\lambda = \sqrt[4]{\frac{\pi^4 EI}{3G\left(\frac{\delta}{t}\right)^2}} \qquad (10)$$

Equation 10 results in a wavelength of approximately 1.3 mm based on a soft resin shear modulus of 1000 psi and T300 fiber properties. The shear modulus was obtained from a Dynamic Mechanical Analyzer (DMA) test conducted on a block of neat DP-7 resin. This wavelength is approximately twice the micro-buckle wavelength estimated from Figure 13. This difference may be attributed to the apparent extreme temperature sensitivity of the resin's shear modulus. A temperature of 95°C would result in a shear modulus that is approximately two and a half times the shear modulus corresponding to 100°C. This 5°C drop in temperature would result in a critical buckle wavelength of approximately 1.0 mm.

Conclusions:

Viscoelastic properties of EMC was determined from tests. Using the elastic properties of a buckled fiber, and the resin's constitutive properties, a model was developed to predict the deployment rate of EMC composites. The model was validated using position and rate data for both slow and rapid deployment rates as may be necessary for actuation of large structures in space.

The deployment performance and repeatability was sufficiently quantified for this EMC laminate. This property is clearly shown to be a function of the induced bending strains. The application of tension during bending was also shown to be a significant contributor to the deployment performance, although the practicality of incorporating tension into a deployment structural system was not investigated.

The analysis portion of the study yielded satisfactory results. An analysis method was devised that allows a materials engineer to obtain an approximation for the maximum achievable curvature a laminate can achieve given any combination of fiber and resin. This was achieved using a combination of kinematic and stability analysis. Additionally, the analysis results were checked with reasonable success using the test results.

During the course of this research the author was also the Principle Investigator of a Space Flight Experiment (EMCH – Elastic Memory Composite Hinge) which was accepted by the Space Experiments Review Board and is scheduled to fly to the International Space Station in 2007.

DETAILED REPORTS:

Further details of the two separate aspects of this report: the 'Deployment rate prediction model' and the 'Deployment Accuracy and Failure study', are available in References 6 and 7, which led the MS and PhD degrees of the respective authors.

References:

1. Beavers, F., Gall, K., Meink, T., Mikulas, M., Munshi, N., and Tupper, M., "Developments in Elastic Memory Composite Materials for Spacecraft Deployable Structures", 2001 IEEE 0-7803-6599-2/01.
2. Findley B., Fundamentals of Composite Manufacturing: Materials, Methods, and Applications. Dearborn: Society of Manufacturing Engineers, 1989.
3. Murphy, T., Meink, T., and Mikalus, M., "Some Micromechanical Considerations of the Folding of Rigidizable Composite Materials", AIAA-2001-1418.
4. Campbel D. and Maji A., "Failure Mechanisms in the Folding of Unidirectional Soft-Resin Composites", Proc. of SEM International Conference, Charlotte, NC, June 2003.
5. Timoshenko, S., Theory of Elastic Stability, McGraw-Hill Book Company, Inc., 1936, pp 109-112.
6. Campbel D., "Deployment Performance of an Elastic Memory Composite", MS Thesis, University of New Mexico, May 2003.
7. Lips J., "Development of a Deployment Rate Prediction Model for Elastics Memory Composites", PhD Dissertation, University of New Mexico, 2006.

ACKNOWLEDGEMENT: